EBioMedicine 59 (2020) 102973

Contents lists available at ScienceDirect

EBioMedicine

journal homepage: www.elsevier.com/locate/ebiom

Plasma metabolomic profiles in liver cancer patients following stereotactic body radiotherapy

Sylvia S.W. Ng[a,b], Gun Ho Jang[c], Irwin J. Kurland[d], Yunping Qiu[d], Chandan Guha[d], Laura A. Dawson[a,b,*]

[a] Radiation Medicine Program, Princess Margaret Cancer Centre, Toronto, ON, Canada
[b] Department of Radiation Oncology, University of Toronto, Toronto, ON, Canada
[c] Division of Bioinformatics, Ontario Institute for Cancer Research, Toronto, ON, Canada
[d] Stable Isotope and Metabolomics Core Facility, Centre for Medical Counter-Measures Against Radiation, Albert Einstein College of Medicine, Bronx, NY USA

ARTICLE INFO

Article History:
Received 1 June 2020
Revised 2 August 2020
Accepted 10 August 2020
Available online xxx

Keywords:
Hepatocellular carcinoma, Stereotactic body radiotherapy
Metabolomics
Biomarkers

ABSTRACT

Background: Stereotactic body radiotherapy (SBRT) is an effective treatment for hepatocellular carcinoma (HCC). This study sought to identify differentially expressed plasma metabolites in HCC patients at baseline and early during SBRT, and to explore if changes in these metabolites early during SBRT may serve as biomarkers for radiation-induced liver injury and/or tumour response.
Methods: Forty-seven HCC patients were treated with SBRT on previously published prospective trials. Plasma samples were collected at baseline and after one to two fractions of SBRT, and analysed by GC/MS and LC/MS for untargeted and targeted metabolomics profiling, respectively.
Findings: Sixty-nine metabolites at baseline and 62 metabolites after one to two fractions of SBRT were differentially expressed, and strongly separated the Child Pugh (CP) B from the CP A HCC patients. These metabolites are associated with oxidative stress and alterations in hepatic cellular metabolism. Differential upregulation of serine, alanine, taurine, and lipid metabolites early during SBRT from baseline was noted in the HCC patients who demonstrated the greatest increase in CP scores at three months post SBRT, suggesting that high protein and lipid turnover early during SBRT may portend increased clinical liver toxicity. Twenty annotated metabolites including fatty acids, glycerophospholipids, and acylcarnitines were differentially upregulated early during SBRT from baseline and separated patients with complete/partial response from those with stable disease at three months post SBRT.
Interpretation: Dysregulation of amino acid and lipid metabolism detected early during SBRT are associated with subsequent clinical liver injury and tumour response in HCC.

1. Introduction

Hepatocellular carcinoma (HCC), the sixth most common cancer globally, carries a poor prognosis. For patients with advanced HCC who are not suitable for local therapies such as surgery or radiofrequency ablation (RFA), external beam radiation therapy is a promising treatment. The liver itself is inherently quite sensitive to radiation. Therefore, care must be taken to ensure that a liver tumour receives the highest dose of radiation at the precise location without causing severe toxicity to the surrounding uninvolved liver and normal luminal gastrointestinal tissues. This is achieved by using stereotactic body radiation therapy (SBRT). Previous studies demonstrated that liver SBRT is well tolerated and effective in Child Pugh (CP) A HCC patients with local control rate of 95% and 85% at 1 year and 3 year, respectively [1–4]. SBRT is also a treatment option for CP B HCC patients, although lower radiation doses are required due to an increased risk of hepatic toxicity [5]. Classic radiation-induced liver disease (RILD), characterized by anicteric ascites, hepatomegaly, occasional right upper quadrant discomfort, and isolated alkaline phosphatase elevation out of proportion to the other liver enzymes within four months of whole or near whole liver radiation, is uncommon following SBRT as hepatic dose-volume constraints are well established to ensure the risk is low [6]. In contrast, non-classic RILD, often manifested as jaundice, general decline in liver function, or marked transaminitis within three months of liver radiation, is not uncommon following HCC SBRT [6], and has been reported in 10-30% of CP A patients and up to 50% of CP B patients post SBRT [1–3,5]. Both classic and non-classic RILD can be life threatening.

Funding: CIHR, NCIC, NCI/NIH, and OICR.
* Corresponding author. .
E-mail address: Laura.Dawson@rmp.uhn.ca (L.A. Dawson).

https://doi.org/10.1016/j.ebiom.2020.102973

Research in context

Evidence before this study

Stereotactic body radiotherapy (SBRT) is an effective treatment option for hepatocellular carcinoma (HCC). Although SBRT is generally well-tolerated, non-classic radiation-induced liver disease still occurs in 10-30% of Child Pugh A HCC patients and up to 50% of Child Pugh B HCC patients post SBRT, and can be life threatening. The known clinical predictor of toxicity and survival such as decline in Child Pugh score is often a comparison between pre-SBRT and 1 to 3 months after completion of SBRT. Hence, there is a strong need to identify biomarkers that can detect radiation-induced liver toxicity early during SBRT for appropriate medical intervention and/or radiation dose reduction and predict tumor response, thereby allowing radiation oncologists to weigh the benefits and risks of SBRT earlier in the patient's treatment course, ideally prior to completion of SBRT.

Added value of this study

This is the first study to demonstrate that dysregulation of amino acid and lipid metabolism early during SBRT (i.e., after only one to two of the planned six fractions) are associated with radiation-induced liver injury and tumor response at three months post treatment in HCC patients.

Implications of all the available evidence

We think that assessing early changes in specific plasma metabolites of amino acid and lipid metabolism during SBRT complements the current clinical predictors and have the potential to further individualize radiation treatment.

Radiation-induced liver toxicity can manifest as fatigue, nausea, increase in abdominal girth, jaundice, or general decline in liver function. When symptoms of liver failure appear, the probability of irreversible organ damage is high. Routine clinical liver function tests do not generally show marked changes after only one to two fractions of SBRT. Consequently, there is a need to identify biomarkers that can detect radiation-induced liver toxicity early for appropriate medical intervention and/or radiation dose reduction and predict tumour response, thereby allowing radiation oncologists to weigh the benefits and risks of SBRT earlier in the patient's treatment course, ideally prior to completion of SBRT. Upon encountering an insult such as radiation, normal or cancer cells modify their use of different biofuels to generate energy and building blocks for repairing the injury [7,8]. Such changes may lead to alterations in the levels of specific plasma metabolites, which can be identified and quantified by gas/liquid chromatography and mass spectrometry [9]. Metabotypes represent the real-time biochemical state of the patient and may be particularly important in HCC, as the liver is the main hub for numerous metabolic and synthetic functions [6]. Detection of distinct metabotypes for SBRT-treated HCC is one strategy towards establishing liver toxicity and tumour response signatures that may help separate patients more likely to develop toxicity and/or have a response to radiation therapy.

In the clinical setting, CP score is used as a surrogate of liver function in patients with chronic liver diseases and to stratify HCC patients in clinical trials [6]. Johnson et al. [10] demonstrated that albumin-bilirubin (ALBI) grade is a more objective and discriminatory metric for the assessment of liver function in HCC patients, without requiring subjective determinants of liver failure such as ascites and encephalopathy. At the cellular/biochemical level, the dysregulation of hepatic cellular metabolic and biosynthetic pathways in HCC following SBRT remains to be elucidated. The primary objective of the current study was to identify differentially expressed plasma metabolites in HCC patients at baseline and following one to two fractions of SBRT and to explore if expression changes in these metabolites are associated with radiation-induced liver toxicity, while the secondary objective was to investigate metabolite association with radiographic tumour response.

2. Materials and methods

2.1. Patients and treatment

The current study was approved by the Research Ethics Board (Oncology)/University Health Network (Toronto, ON, Canada). Plasma samples were obtained from locally advanced HCC patients who participated in two previously published prospective clinical trials [1,5]. Written informed consent was obtained from patients. Briefly, eligible patients had HCC who were unsuitable for transplant, resection, RFA or transcatheter arterial chemoembolization, CP A with maximum individual tumour size of 15 cm or CP B with maximum tumour size of 10 cm, 5 or fewer liver tumours, and 700 cc of uninvolved liver. The presence of portal vein tumour thrombosis or prior therapies were permitted. The patients were treated to a dose of 30 to 54 Gy in 6 fractions every other day. Patients were instructed not to intake anything by mouth other than water for at least 2 h prior to each radiation fraction. Although treatments were not required to be at exactly the same time each day, they tended to occur at a similar time of day for each patient's course of SBRT. Patients who consented to participation in the aforementioned published prospective clinical trials were eligible to also consent to plasma sample collection at baseline and after having received one to two of the 6 fractions of SBRT. Fasting was not a prerequisite for each blood draw. The collected plasma samples were stored at −80 °C until the time of analysis.

2.2. Evaluation of clinical parameters

Increase in CP score, which signifies decline in liver function, at three months post SBRT compared to baseline in the absence of tumour progression was used as a surrogate for liver toxicity, and categorized into two groups: less than two points increase and two or more points increase. Radiographic in-field tumour response at three months post SBRT was assessed using RECIST version 1·1 [11].

2.3. Identification and quantification of plasma metabolites

Gas chromatography/mass spectrometry (GC/MS) and liquid chromatography/mass spectrometry (LC/MS) studies were performed for untargeted and targeted metabolomics profiling, respectively, in the Stable Isotope and Metabolomics Core Facility of the Albert Einstein College of Medicine. The untargeted GC/MS assay detected many small metabolites well, especially organic acids and microbiome-related metabolites, and allowed a more global scanning of the metabolome. The targeted LC/MS assay, which used the commercially available Biocrates Absolute*IDQ* p180 kit (Biocrates Inc., Washington, DC) to assess over 180 known metabolites that are categorized into 5 classes – acylcarnitines, amino acids, glycerophospholipids, sphingolipids, and biogenic amines, focused on specific metabolites in a more quantitative fashion. See Supplementary Materials for more information on the GC/MS and LC/MS assays. Metabolites annotation was performed by comparing the mass spectrum and retention time to commercially available libraries such as Fiehn library, GOLM libraries, and NIST library. Non-annotated metabolites are those metabolites that were detectable with GC/MS but whose mass spectrum and

retention time do not match to those of known metabolites in the commercially available libraries.

2.4. Metabolomic data analysis and statistics

GC/MS and LC/MS data were log transformed and subtracted median expression of each metabolite for downstream analysis. In differential expression analyses, fold change was computed by taking exponential of the difference between median expression of the two groups (baseline *vs.* after one to two fractions of SBRT). The "high" or "low" was determined if the fold change is greater or less than one, respectively. Some subclasses had small number of samples which resulted in inaccurate statistical tests. As such, three statistical tests (Anderson-Darling test, Wilcoxon rank sum test, Kolmogorov-Smirnov test) were used and the metabolites with *p*-values $\leq$0·05 in all three tests were selected as metabolites of interest. To control false positive rate, two layers of corrections were applied. First, the Benjamini-Hocheberg method [12] was applied to the *p*-values from each of the aforementioned statistical tests. Second, potential dependency of three q-values was corrected using the Benjamini-Yekutieli method [13] for each metabolite. These conservative selection criteria were set for metabolites of interest rather than using only one test so potential metabolites were not missed given the exploratory and hypothesis generating nature of this study. Increase in CP score was dichotomized into less than two points vs. two or more points, while radiographic tumour response was dichotomized into response (complete or partial response) vs. no response (stable disease), applying the aforementioned differential expression analyses with statistical significance set at all three p-values $\leq$0·05.

2.5. Metabolite set enrichment analysis (MSEA)

To identify biologically meaningful patterns, over representation and pathway analyses were performed on the differentially abundant metabolites after one to two fractions of SBRT using MetaboAnalyst 4·0 (www.metaboanalyst.ca). The hypergeometric test was utilized in the over representation analysis to determine whether a particular metabolite set is represented more than expected by chance within the given list of metabolites. One-tailed p-values were provided after adjusting for multiple testing (www.metaboanalyst.ca).

Table 1
Patient and Treatment Characteristics.

Variable	Number of patients (%)	Median (range)
Age		70 (48-90)
Gender		
Male	37 (79%)	
Female	10 (21%)	
Cause of underlying chronic liver disease		
Alcohol	22 (47%)	
Hepatitis B	13 (28%)	
Hepatitis C	22 (47%)	
Non-alcoholic steatohepatitis	2 (4%)	
Child Pugh score		
A5	27 (57%)	
A6	11 (24%)	
B7	9 (19%)	
ALBI grade		
1	20 (43%)	
2	24 (51%)	
3	3 (6%)	
HCC thrombus		
Absent	21 (45%)	
Present	26 (55%)	
Previous Treatment		
Any	23 (49%)	
None	24 (51%)	
In-field tumor response at 3 months post SBRT		
Stable disease	21 (45%)	
Partial response	15 (32%)	
Complete response	1 (2%)	
Unknown	10 (21%)	
Baseline laboratory values		
Bilirubin, μmol/L		14 (6-42)
Albumin, g/L		38 (23-47)
Platelet, $\times$ 10^9/L		117 (55-366)
Gross tumor volume, mL		96.8 (1.3-1385.1)
Prescription dose, Gy		33 (30-54)
Liver mean dose, Gy		15.3 (4.3-18.2)
D800cc, Gy		7.4 (0-25.3)
Veff, %		39 (9-60)
Liver volume, mL		1231.4 (750-3080.7)

3. Results

This study included 38 of 102 CP A and 9 of 29 CP B patients from two previous published prospective clinical trials [1,5] because these patients provided plasma samples at baseline and after having received one to two of six fractions of SBRT. The patient and treatment characteristics are listed in Table 1. In-field tumour response at three months post SBRT was available for 31 of 38 CP A patients, and 6 of 9 CP B patients due to death or absence of imaging.

3.1. Differential expression of metabolites by CP score at baseline and after SBRT

At baseline, 69 metabolites of interest were differentially expressed (all three *p*-values $\leq$0·05) in HCC patients and strongly separated the CP B patients from the CP A patients (Fig. 1a); 54 of the 69 metabolites are annotated and have known identities. Interestingly, one CP A patient (H071) clustered more closely with the CP B patients than the remaining CP A patients. Nineteen metabolites including specific acylcarnitines and glycerophospholipids, and two metabolites including lyso PC a C26:1 and uracil were consistently detected at higher and lower levels in the CP B patients, respectively, than in the CP A patients both at baseline and following one to two fractions of SBRT (Tables 2 and 3). After subtracting the shared metabolites for high and low expression between the two time points, 13 unique metabolites such as numerous acylcarnitines and SDMA were expressed at higher levels, while 20 unique metabolites such as alanine, isoleucine, valine, sarcosine, 2-ketoisocaproic acid, and several glycerophospholipids and lysophospholipids were expressed at lower levels in the CP B than in the CP A HCC patients at baseline (Table 2). MSEA of the high expressing metabolites showed impairment of fatty acid oxidation, resulting in increases in acylcarnitines associated with elevations of phospholipids whose fatty acid side chains are not being utilised (Fig. 1b). MSEA of the low expressing metabolites demonstrated that degradation of amino acids, especially branched chain amino acids (BCAAs), may be responsible for the observed decreases in amino acid levels, evidenced by the lower level of the BCAA metabolite 2-ketoisocaproic acid, which may indicate accelerated disposal of BCAAs (Fig. 1c). Furthermore, the enrichment node connections in Fig. 1c illustrated the inter-relationship between methionine and glycine/serine metabolism, suggesting the importance of sarcosine which links these pathways to phosphatidylcholine metabolism. When the *q*-value $<$0·1 criterion was applied, only 5 annotated metabolites were significantly differentially expressed and strongly separated the CP 7 patients from the CP A patients (Table 2). One unique metabolite, C6:1, was expressed at significantly higher level, while 2 unique metabolites including PC aa C24:0 and sarcosine were expressed at significantly lower levels in the CP B than in the CP A HCC patients at baseline (Table 2 and Supplementary Fig. S2a).

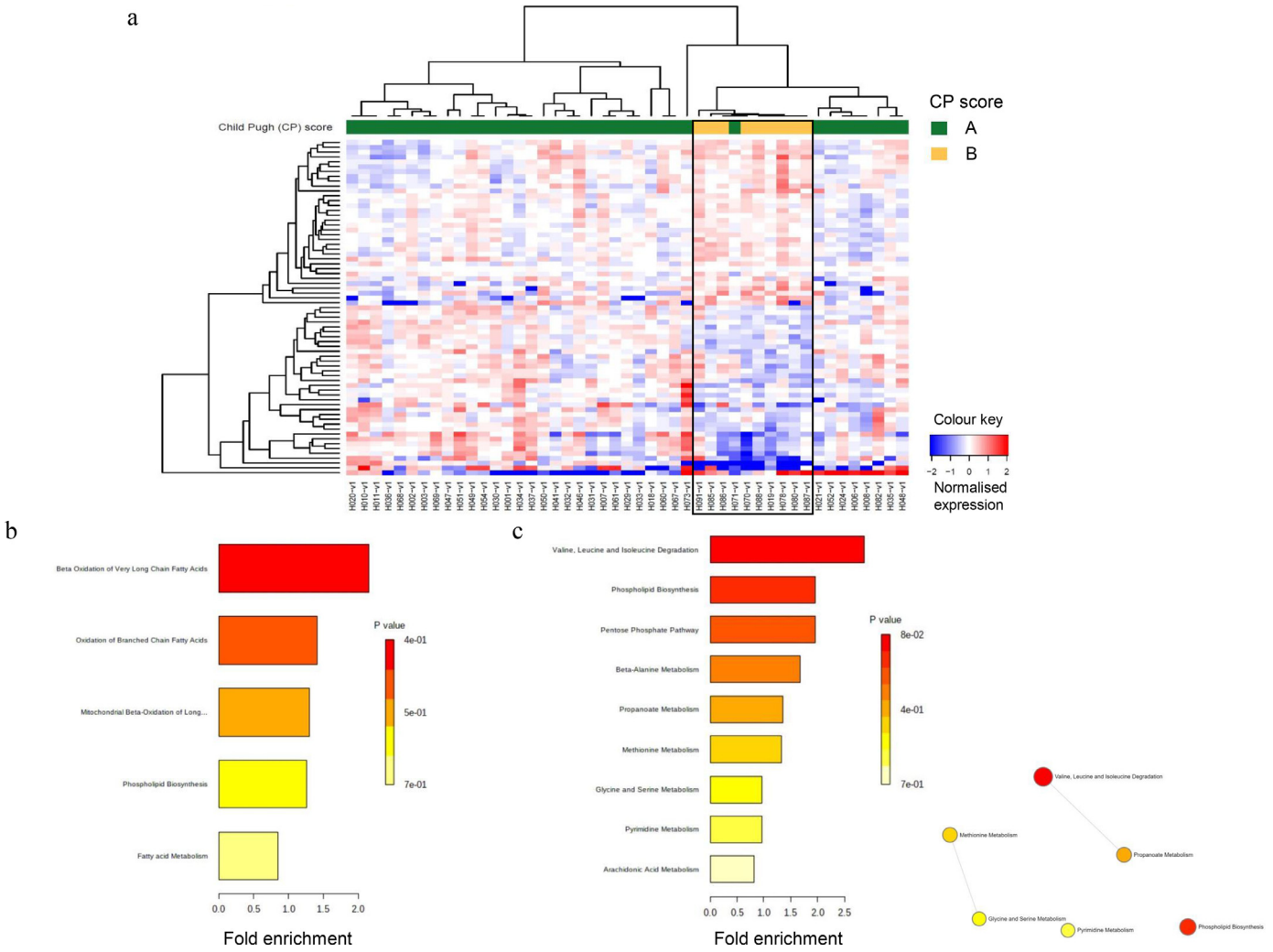

Fig. 1. Differential expression of metabolites in HCC patients at baseline. (a) Heatmap showing differentially expressed (all three p-values ≤0·05) plasma metabolites by Child Pugh (CP) scores, A (green) and B (yellow). Each column represents a patient; each row represents an individual metabolite. The more intense the red colour, the higher the level of the metabolite was detected. The more intense the blue colour, the lower the level of the metabolite was detected. See Table 2 for the identities of the annotated metabolites. (b) Metabolic set enrichment analysis (MSEA) of the high expressing metabolites. (c) MESA and enrichment node connections of the low expressing metabolites. Each node represents a metabolite set with its colour based on the P value, and its size is based on the fold enrichment for the metabolite list in query. Two metabolite sets are connected by an edge if the number of combined metabolites is over 20% the number of their combined metabolite sets.

After one to two fractions of SBRT, 62 metabolites of interest were differentially expressed (all three *p*-values ≤0·05) and strongly separated the CP B patients from the CP A patients (Fig. 2a), of which 46 are annotated. Five CP A patients (H071, H069, H068, H061, H035) clustered more closely with the CP B patients than the remaining CP A patients after one to two fractions of SBRT. Twenty-five unique metabolites, including citrulline, taurine, tyrosine, glycolic acid, N-methyl-glutamic acid 1, and specific phosphatidylcholines, were detected at higher levels, while no unique metabolites were expressed at lower levels in CP B vs. CP A HCC patients following one to two fractions of SBRT (Table 3). MSEA and enrichment node connections of the high expressing metabolites are summarized in Fig. 2b, demonstrating the significance of taurine, phosphatidylinositol phosphate and inositol phosphate metabolism; and the inter-relationships between amino acid/nicotinate-nicotinamide metabolism and urea cycle, and between inositol and inositol phosphate metabolism. When the *q*-value <0·1 criterion was applied, only 18 annotated metabolites were significantly differentially expressed that strongly separated the CP B patients from the CP A patients (Table 3 and Supplementary Fig. S2b). Seven unique metabolites including citrulline, PC aa C30:0, PC ae C30:0, PC ae C34:0, PC ae C34:2, PC ae C38:5, and PC ae C42:3 were expressed at significantly higher levels, while no unique metabolites were expressed at lower levels in the CP B than in the CP A HCC patients after one to two fractions of SBRT (Table 3 and Supplementary Fig. S2b). Differential expression analysis of metabolites by ALBI grade at baseline and after SBRT were also performed and included in Supplementary Results.

3.2. Dysregulation of metabolites after one to two fractions of SBRT from baseline in relation to increase in CP score at three months post SBRT

As shown in Fig. 3a, 41 metabolites of interest showed differential expression changes (all three *p*-values ≤0·05) between baseline and following one to two fractions of SBRT when increase in CP score at three months post SBRT was analysed. Of the 41 metabolites, 13 are annotated (Table 4). Differential upregulation of 4-deoxypyridoxine (1·30-fold), alanine (1·32-fold), arachidonic acid (1·25-fold), C3 (1·52-fold), creatinine (1·25-fold), lysoPC a C24:0 (1·23-fold), oxalic acid (1·12-fold), pipecolic acid (1·12-fold), pyroglutamic acid (1·25-fold), serine (1·27-fold), taurine (1·24-fold), trans-3-hydoxy-L-proline (1·36-fold), and xylitol (1·27-fold) after one to two fractions of SBRT was seen in the HCC patients who subsequently demonstrated the greatest increase in CP score (two or more points) at three months post SBRT (Fig. 3b). Interestingly, three CP A patients (H071, H068,

Table 2
Annotated plasma metabolites that were differentially expressed (all three p-values ≤0·05) at higher or lower levels in Child Pugh B (CP B) vs. Child Pugh A (CP A) HCC patients at baseline. The p-values presented are from the Wilcoxon rank sum test. Metabolites with all three p-values ≤0·05 and q-value ≤0·1 are marked [‡]. Metabolites identified by GC/MS are marked [#], while those identified by LC/MS are not marked.

AT BASELINE							
High expressing metabolites in CP B vs. CP A				Low expressing metabolites in CP B vs. CP A			
Identity[†]	Fold diff[*]	p-value	q-value	Identity[†]	Fold diff[*]	p-value	q-value
C10	1·29	0·017	0·41	2-ketoisocaproic acid[#]	0·67	0·002	0·16
C10:1	1·39	0·007	0·30	Alanine	0·69	0·0007	0·11
C12	1·27	0·014	0·40	Decanoic acid	0·88	0·008	0·24
C12:1	1·45	0·002	0·15	Isoleucine	0·64	0·017	0·42
C14	1·26	0·011	0·35	Gluconic acid lactone[#]	0·67	0·046	0·50
C14:1-OH	1·49	0·001	0·12	LysoPC a C14:0	0·91	0·010	0·34
C14:2-OH	1·58	0·0007	0·11	LysoPC a C16:0	0·65	0·012	0·37
C16	1·48	0·003	0·21	LysoPC a C16:1	0·59	0·010	0·35
C16:1	1·76	0·001	0·14	LysoPC a C18:2	0·72	0·019	0·45
C16:2	1·45	0·042	0·49	LysoPC a C20:3	0·70	0·026	0·37
C18	1·40	0·044	0·49	LysoPC a C20:4	0·67	0·047	0·50
C18:1	1·66	0·0006	0·11	LysoPC a C26:0	0·64	0·0009	0·12
C18:2	1·50	0·0004	0·24	LysoPC a C26:1	0·62	0·005	0·24
C2	1·60	0·014	0·40	LysoPC a C28:0	0·64	0·001	0·12
C5:1-DC	1·35	0·021	0·48	PC aa C24:0	0·64	3·96E-05	0·008[‡]
C6:1	1·83	0·0002	0·04[‡]	PC aa C26:0	0·70	0·002	0·11
PC aa C32:0	1·64	0·0008	0·09[‡]	PC aa C32:3	0·72	0·030	0·50
PC aa C40:2	1·23	0·012	0·37	PC aa C34:4	0·60	0·007	0·22
PC aa C42:0	1·31	0·011	0·25	PC aa C36:4	0·68	0·039	0·50
PC aa C42:4	1·21	0·026	0·50	Sarcosine	0[§]	3·72E-05	<0·001[‡]
PC ae C32:1	1·54	7·46E-05	0·033[‡]	Uracil[#]	0·63	0·003	0·21
PC ae C32:2	1·19	0·016	0·42	Valine	0·81	0·009	0·33
PC ae C34:1	1·41	0·019	0·15				
PC ae C34:3	1·27	0·032	0·41				
PC ae C36:0	1·29	0·036	0·48				
PC ae C42:4	1·33	0·004	0·23				
PC ae C42:5	1·20	0·008	0·31				
PC ae C44:5	1·29	0·017	0·37				
PC ae C44:6	1·31	0·013	0·40				
SDMA	1·75	0·002	0·14				
SM C16:0	1·22	0·013	0·35				
SM C26:1	1·33	0·005	0·24				

[*] Fold diff, fold difference between CP B vs. CP A HCC patients.
[†] C10, decanoylcarnitine; C10:1, decenoylcarnitine; C12, dodecanoylcarnitine; C12:1, dodecenoylcarnitine; C14, tetradecanoylcarnitine; C14:1-OH, hydroxytetradecenoylcarnitine; C14:2-OH, hydroxytetradecadienylcarnitine; C16, hexadecanoylcarnitine; C16:1, hexadecenoylcarnitine; C16:2, hexadecadienylcarnitine; C18, octadecanoylcarnitine; C18:1, octadecenoylcarnitine; C18:2, octadecadienylcarnitine; C2, acetylcarnitine; C5:1-DC, glutaconylcarnitine, C6:1, hexenoylcarnitine; PC aa, phosphatidylcholine diacyl, PC ae, phosphatidylcholine acyl-alkyl; SDMA, symmetric dimethyl arginine; SM, sphingomyelin.
[‡] Metabolites with all three p-values ≤0·05 and q-value <0·1.
[§] There was no expression of sarcosine in CP B HCC patients. As such, when dividing no expression in CP B patients by some expression in CP A HCC patients, the fold difference appeared as 0.
[#] Metabolites identified by GC/MS. Metabolites identified by LC/MS are not marked.

H035), who clustered most closely with the CP B patients after one to two fractions of SBRT, had the greatest increase in CP score at three months post SBRT (Fig. 2a and Fig. 3a). When the *q*-value <0·1 criterion was applied, no annotated metabolites demonstrated significant differential expression changes that separated the HCC patients with increase in CP score of two or more points from those of less than two points at three months post SBRT.

3.3. Dysregulation of metabolites after one to two fractions of SBRT from baseline in relation to tumour response at three months post SBRT

As shown in Fig. 4a, 25 metabolites of interest showed differential expression changes (all three *p*-values ≤0·05) between baseline and after one to two fractions of SBRT when in-field tumour response on imaging at three months post SBRT was analysed. Of the 25 metabolites, 20 are annotated (Fig. 4a). All 20 annotated metabolites were differentially upregulated. For instance, differential upregulation of 3-hydroxybutyric acid (2·36-fold), C16:1 (1·41-fold), C6 (C4:1-DC) (1·33-fold), and PC aa C40:4 (1·17-fold) after one to two fractions of SBRT were observed in the HCC patients with complete/partial response compared to those with stable disease at three months post SBRT (Fig. 4b). When the q-value <0·1 criterion was applied, no metabolites demonstrated significant expression changes that separated the HCC patients with response (complete/partial) from those with no response (stable disease) at three months post SBRT.

4. Discussion

Our study demonstrated that at baseline, unique plasma lipid and protein metabolites are differentially expressed at higher or lower levels in CP B vs. CP A and in ALBI grade 2/3 vs. grade 1 HCC patients, reflecting the changes in both non-cancerous and cancerous hepatocellular anabolic/catabolic need as the severity of liver impairment increases secondary to the worsening of chronic liver disease and/or the presence of malignancy. High levels of circulating acylcarnitines in the CP B HCC patients might be explained by the failure of their transport into the mitochondrial matrix as liver function declines, resulting in the switch from mitochondrial to peroxisomal fatty acid oxidation and the production of hydrogen peroxide, which causes further liver damage [14,15].

Table 3
Annotated plasma metabolites that were differentially expressed (all three p-values ≤0·05) at higher or lower levels in Child Pugh B (CP B) vs. Child Pugh A (CP A) HCC patients after one to two fractions of liver SBRT. The p-values presented are from the Wilcoxon rank sum test. Metabolites with all three p-values ≤0·05 and q-value ≤0·1 are marked [‡]. Metabolites identified by GC/MS are marked [#], while those identified by LC/MS are not marked.

AFTER 1 TO 2 FRACTIONS OF SBRT							
High expressing metabolites in CP B vs. CP A				Low expressing metabolites in CP B vs. CP A			
Identity[†]	Fold diff[*]	p-value	q-value	Identity[†]	Fold diff[*]	p-value	q-value
C14:1-OH	1·20	0·021	0·42	LysoPC a C26:1	0·52	0·001	0·090[‡]
C14:2-OH	1·55	0·012	0·24	Uracil[#]	0·61	0·003	0·12
C16:1	1·39	0·032	0·43				
C16:1-OH	1·29	0·022	0·42				
C5:1-DC	1·39	0·008	0·27				
Citrulline[#]	1·96	0·0004	0·081[‡]				
Glycolic acid[#]	1·17	0·046	0·53				
Myo-inositol[#]	1·66	0·030	0·43				
Nicotinic acid[#]	3·07	0·022	0·33				
N-methyl-glutamic acid 1[#]	1·25	0·049	0·54				
PC aa C30:0	1·68	0·0005	0·081[‡]				
PC aa C32:0	1·64	4·98E-05	0·004[‡]				
PC aa C34:1	1·33	0·009	0·32				
PC aa C36:1	1·32	0·003	0·15				
PC aa C40:2	1·26	0·002	0·12				
PC aa C42:0	1·25	0·003	0·15				
PC aa C42:4	1·20	0·006	0·17				
PC ae C30:0	1·53	0·0002	0·076[‡]				
PC ae C32:1	1·59	1·82E-05	<0·001[‡]				
PC ae C32:2	1·38	0·0006	0·084[‡]				
PC ae C34:0	1·55	0·001	0·092[‡]				
PC ae C34:1	1·58	0·0002	0·004[‡]				
PC ae C34:2	1·49	0·0005	0·081[‡]				
PC ae C34:3	1·52	0·0003	0·076[‡]				
PC ae C36:0	1·51	0·001	0·092[‡]				
PC ae C36:2	1·27	0·005	0·19				
PC ae C36:3	1·34	0·002	0·12				
PC ae C36:4	1·27	0.011	0·36				
PC ae C38:2	1·18	0·004	0·20				
PC ae C38:5	1·45	0·002	0·086[‡]				
PC ae C40:5	1·34	0·005	0·12				
PC ae C42:2	1·20	0·007	0·27				
PC ae C42:3	1·44	0·001	0·092[‡]				
PC ae C42:4	1·34	0·001	0·081[‡]				
PC ae C42:5	1·31	0·003	0·092[‡]				
PC ae C44:3	1·17	0·006	0·25				
PC ae C44:5	1·30	0·006	0·24				
PC ae C44:6	1·43	0·007	0·27				
SM (OH) C24:1	1·36	0·011	0·34				
SM C16:0	1·27	0·001	0·081[‡]				
SM C24:1	1·15	0·012	0·36				
SM C26:1	1·33	0·001	0·092[‡]				
Taurine	1·50	0·008	0·23				
Tyrosine	1·52	0·010	0·37				

[*] Fold diff, fold difference between CP B vs. CP A HCC patients.
[†] C14:1-OH, hydroxytetradecenoylcarnitine; C14:2-OH, hydroxytetradecadienylcarnitine; C16:1, hexadecenoylcarnitine; C16:1-OH, hydroxyhexadecenoylcarnitine; C5:1-DC, glutaconylcarnitine; LysoPC a, lysophosphatidylcholine acyl, PC aa, phosphatidylcholine diacyl, PC ae, phosphatidylcholine acyl-alkyl; SM, sphingomyelin.
[‡] Metabolites with all three p-values ≤0·05 and q-value <0·1.
[#] Metabolites identified by GC/MS. Metabolites identified by LC/MS are not marked.

Previous studies reported that the serum levels of most lipids are decreased in HCC patients compared to hepatitis patients, cirrhotic patients, and healthy controls [16–19]. Decreased serum levels of phosphatidylcholines in HCC patients appeared to be associated with increased hepatocellular tumour levels of phosphatidylcholines, which is thought to be the result of their uptake from serum into hepatocellular tumour cells for cellular membrane biosynthesis, signalling, and cell cycle progression [17,20]. The depletion of circulating lysophosphatidylcholines in HCC patients might be attributed to their increased catabolism to lysophosphatidic acids by extracellular lysophospholipase D [18,21]. Our data further showed that HCC patients with poorer liver function (CP B, ALBI grade 2/3) differentially expressed lower plasma levels of multiple lysophosphatidylcholines than those with better liver function (CP A, ALBI grade 1).

Following only one to two fractions of SBRT, higher plasma levels of the glycerophospholipids such as PC aa C30:0 and PC ae C30:0 were detected in the HCC patients with higher baseline CP score and ALBI grade compared to their lower score/grade counterparts, suggesting increased radiation-induced lipid turnover in the impaired livers. In line with our findings, some preclinical studies previously demonstrated significant dysregulation of various glycerophospholipids in the liver of non-human primates and rats at early (3 days) and late (60 days) time points following a single dose of whole body irradiation (which included the whole liver) compared to that of healthy controls who did not receive whole body irradiation [22,23]. Dysregulation of glycerophospholipids has also been reported in prostate cancer patients who developed urinary symptoms following prostate SBRT [24]. The differential up- and down-regulation of lipid species

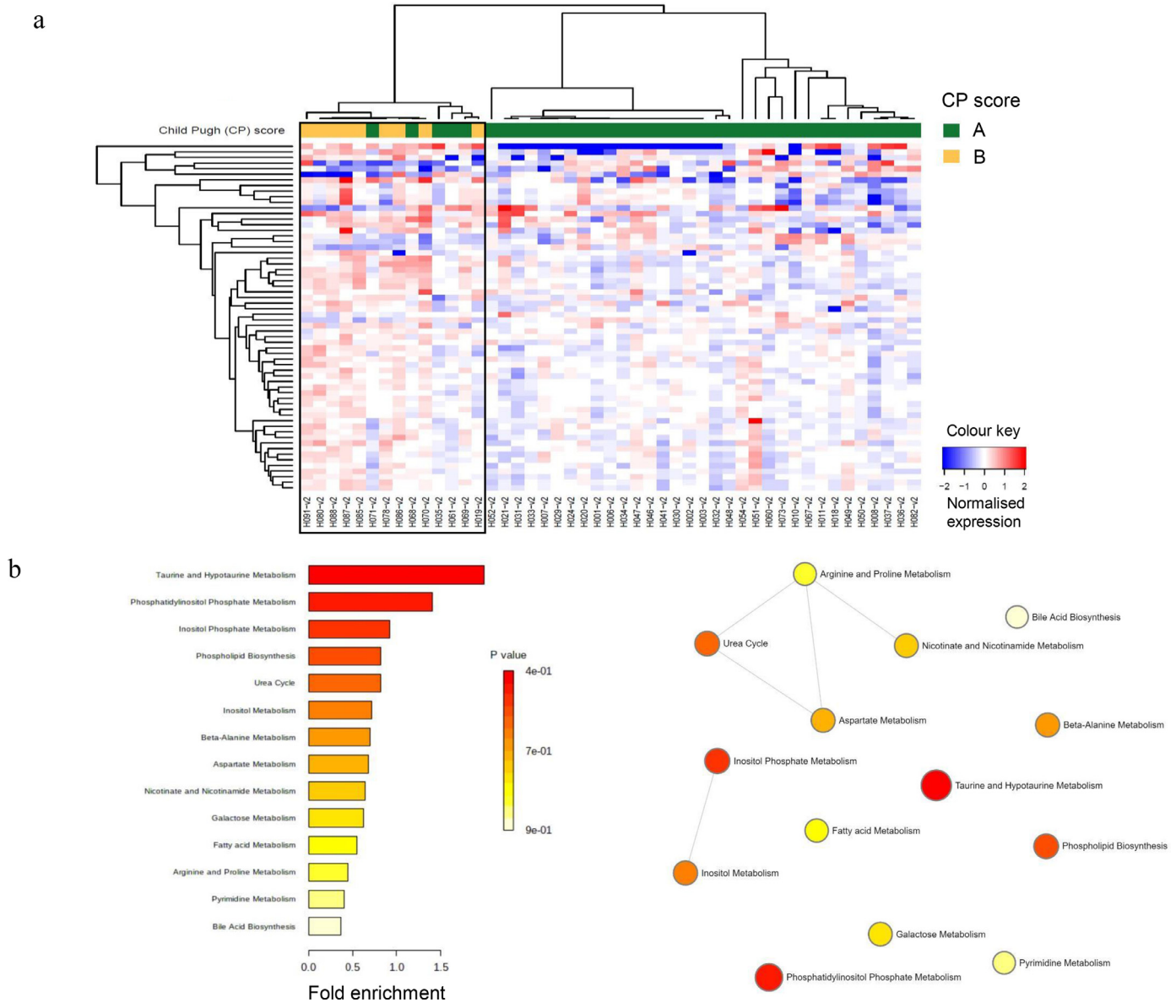

Fig. 2. Differential expression of metabolites in HCC patients following one to two fractions of SBRT. (a) Heatmap showing differentially expressed (all three p-values ≤0·05) plasma metabolites by Child Pugh (CP) scores, A (green) and B (yellow). Each column represents a patient; each row represents an individual metabolite. The more intense the red colour, the higher the level of the metabolite was detected. The more intense the blue colour, the lower the level of the metabolite was detected. See Table 3 for the identities of the annotated metabolites. (b) MESA and enrichment node connections of the high expressing metabolites. Each node represents a metabolite set with its colour based on the P value, and its size is based on the fold enrichment for the metabolite list in query. Two metabolite sets are connected by an edge if the number of combined metabolites is over 20% the number of their combined metabolite sets.

early during liver SBRT in HCC patients may be attributed to the combined effects of early injury to normal hepatocytes from the low dose splash and killing of liver cancer cells from the high dose ablation. Interestingly, phosphatidylcholine was also found to be one of the metabolites being affected following RFA [25]. Taken together, local therapies such as SBRT and RFA appear to increase hepatic lipid turnover, which may be related to cellular damage and lipid release following injury from these treatments. It is well known that phosphatidylcholines play a crucial role in maintaining cell membrane integrity, mediating cellular energy utilization and signal transduction, all of which are required for cell cycle progression and cell survival [20].

Higher levels of amino acids, including citrulline and tyrosine, were detected following only one to two fractions of SBRT in the HCC patients with higher baseline CP score and ALBI grade compared to their lower score/grade counterparts, implicating higher protein turnover via inter-connected pathways of amino acid metabolism in the more fragile livers. Elevated citrulline, which is a part of the urea cycle, in the CP B HCC patients after SBRT might be an indicator of increased toxic load of ammonia secondary to impaired liver function. When evaluating the increase in CP score at three months post SBRT as a surrogate for radiation-induced liver toxicity, early upregulation of serine and alanine were seen in HCC patients with the greatest increase in CP score (two points or more). Increased serine levels might reflect increased glycolysis, as serine can act as an allosteric activator of pyruvate kinase 2 which is involved in the rate limiting step of converting phosphoenolpyruvate to pyruvate [14,15]. As asparagine is anapleurotic to the tricarboxylic acid cycle, and serine and alanine are in equilibrium with pyruvate, this may suggest inadequate mitochondrial compensation and possibly higher protein turnover rate early during SBRT, both of which may portend clinical liver toxicity. Preclinical studies in rats have previously demonstrated

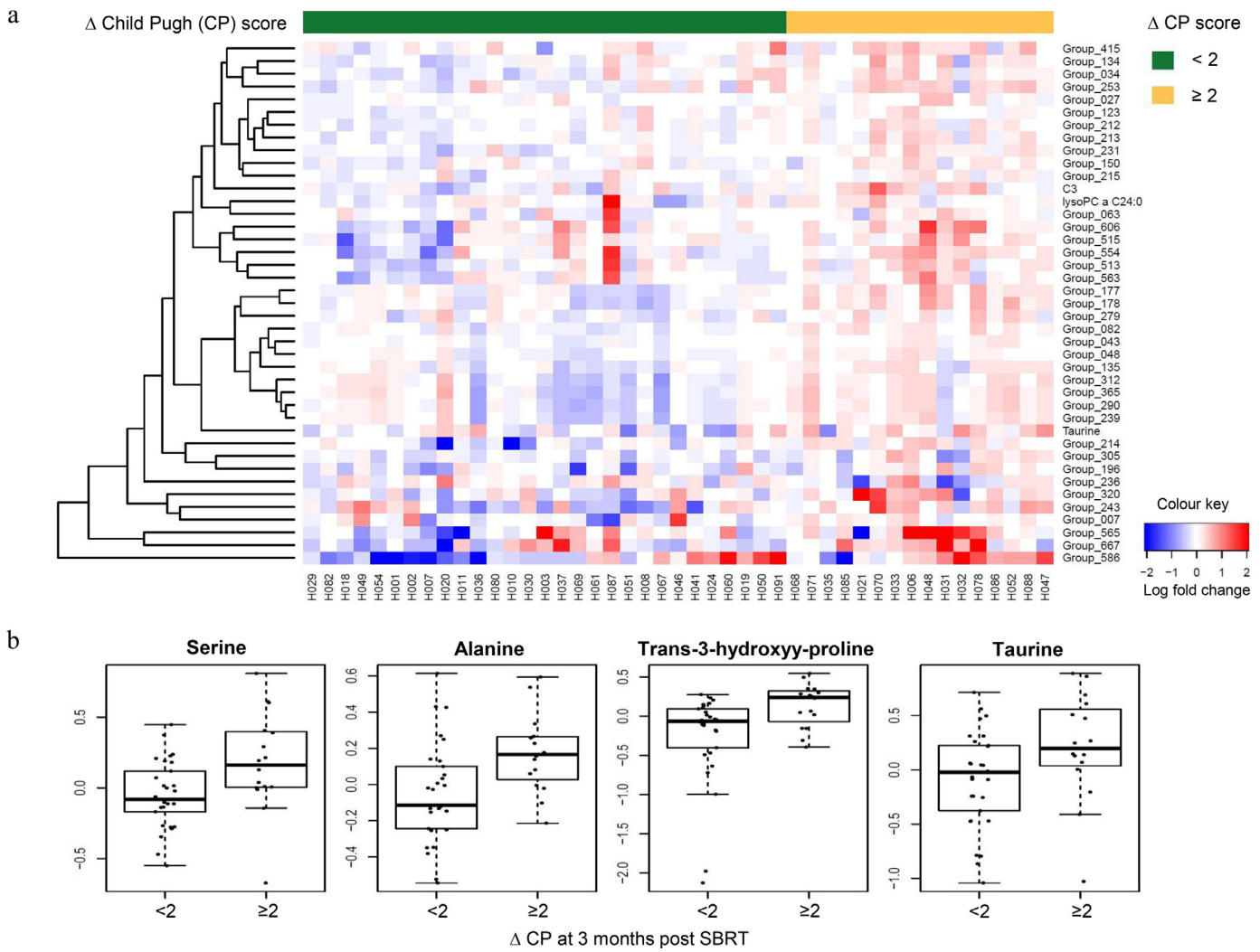

Fig. 3. Differential expression changes of metabolites after one to two fractions of SBRT from baseline by change in Child Pugh (CP) score at three months post SBRT. (a) Heatmap of differential upregulation or downregulation (all three p-values ≤0·05) of plasma metabolites with increase in Child Pugh (ΔCP) score of <2 (green) vs. ≥2 (yellow) points at three months post SBRT compared to baseline. Each column represents a patient. Each row represents an individual metabolite. The more intense the red colour, the higher the level of the metabolite was detected. The more intense the blue colour, the lower the level of the metabolite was detected. See Table 4 for the identities of the annotated metabolites. (b) Representative boxplots showing the fold change of 4 metabolites plotted against increasing ΔCP score at three months post SBRT.

Table 4
Identities of the 13 annotated plasma metabolites of interest on the heatmap in Fig. 3a, all of which showed differential upregulation (all three p-values ≤0·05) after one to two fractions of SBRT from baseline and separated HCC patients by change in Child Pugh (CP) score at three months post SBRT.

Abbreviation	Identity
Group_290	4-deoxypyridoxine
Group_034	Alanine
Group_515	Arachidonic acid
C3	C3*
Group_231	Creatinine
LysoPC a C24:0	LysoPC a C24:0
Group_043	Oxalic acid
Group_123	Pipecolic acid
Group_213	Pyroglutamic acid
Group_134	Serine
Taurine	Taurine
Group_214	Trans-3-hydroxyl-L-proline
Group_305	Xylitol

* C3, propionylcarnitine.

dysregulation of serine and alanine metabolism in the liver of mice after 6 Gy of whole body irradiation [23], consistent with our findings. Early increase in the expression of hydroxyproline, a marker for liver fibrosis [26], was also observed in HCC patients with the greatest decline in liver function at three months post SBRT in the current study. Taken together, upregulation of amino acids secondary to high protein turnover early during SBRT appears to be associated with radiation-induced liver toxicity at a later time.

With respect to potential markers for tumour response to SBRT, increased expression of fatty acids, glycerophospholipids, and acylcarnitines were noted after one to two fractions from baseline in patients with response (complete/partial) compared to those with no response (stable disease) at three months post SBRT. 2-hydroxybutyric acid takes part in the metabolism of multiple amino acids such as methionine and threonine. Elevated levels of 2-hydroxybutyric acid may reflect early protein turnover and release of amino acids for metabolism in patients who demonstrated complete/partial response to SBRT. In the same vein, increased levels of various fatty acids may suggest early membrane damage and subsequent cell death in the responders post SBRT. The implication of these metabolites in the context of HCC remains to be elucidated.

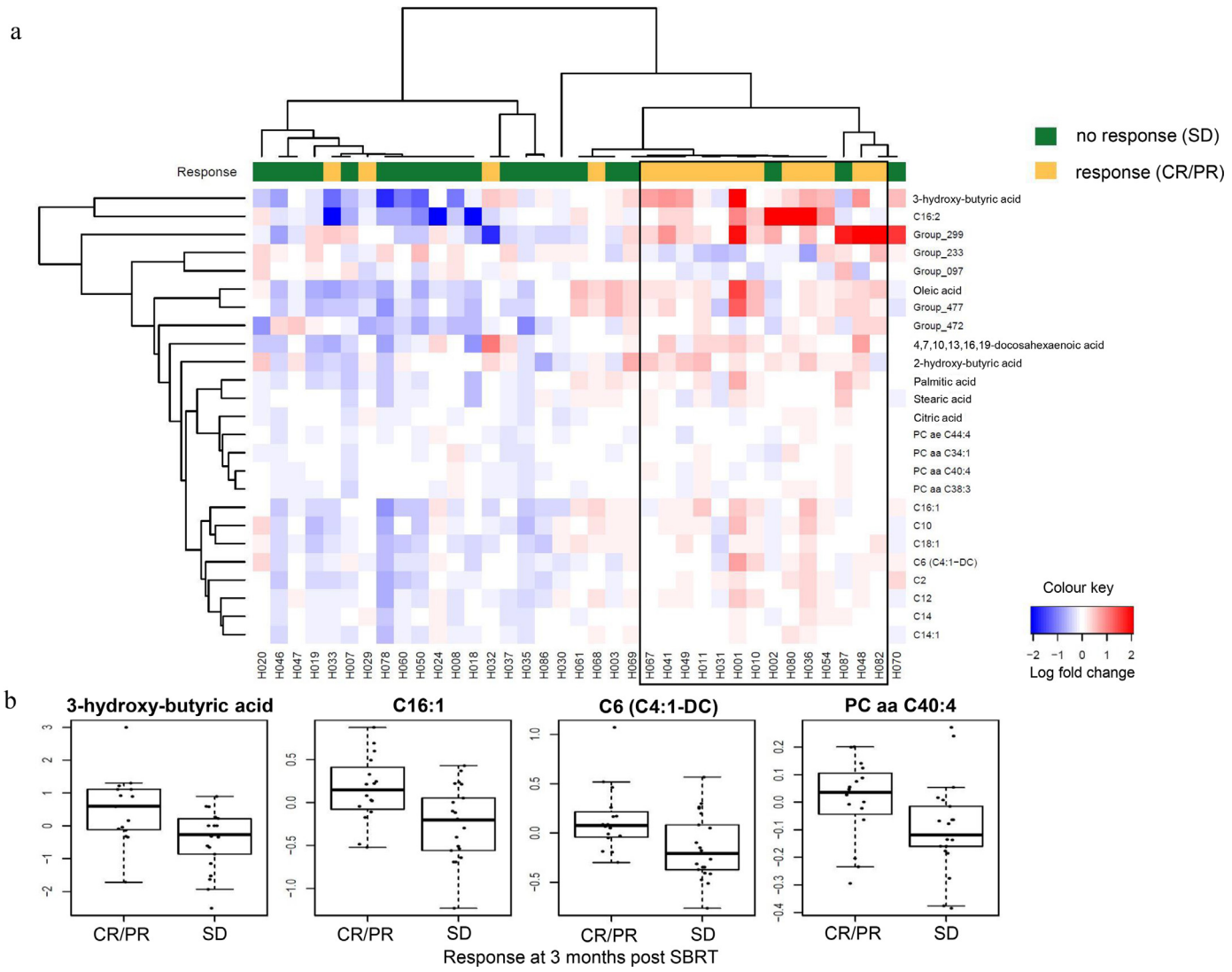

Fig. 4. Differential expression changes of metabolites after one to two fractions of SBRT from baseline by in-field tumour response at three months post SBRT. (a) Heatmap of differential upregulation or downregulation (all three p-values ≤0·05) of plasma metabolites in HCC patients with response (complete/partial, CR/PR, yellow) vs. those with no response (stable disease, SD, green) at three months post SBRT. Each column represents a patient. Each row represents an individual metabolite. The more intense the red colour, the higher the level of the metabolite was detected. The more intense the blue colour, the lower the level of the metabolite was detected. (b) Representative boxplots showing the fold change of 4 metabolites plotted against in-field tumour response at 3 months post SBRT.

To our knowledge, this is the first study to demonstrate that early dysregulation of amino acid and lipid metabolism during SBRT are associated with radiation-induced liver injury and tumour response at three months post treatment in HCC patients. This study is exploratory and hypothesis-generating, with the limitations of small sample size and absence of a validation cohort. However, conservative statistical criteria were used to select strongly related metabolites. It should be noted that plasma levels of metabolites are influenced by feeding or fasting, and no straight dietary restrictions were imposed on our patient cohort. The utility of the identified metabolites as surrogate biomarkers for clinical liver toxicity and tumour response and/or mitigating agents warrants further in-depth prospective evaluation in future trials that are statistically powered based on the magnitude of difference detected in the current study.

Funding

This work was supported by the Canadian Institutes of Health Research (Grant #202477), National Cancer Institute of Canada (Grant #18207), and the National Cancer Institute/National Institutes of Health (Grant #P60DK020541) for the Stable Isotope and Metabolomics Core Facility, Diabetes Research and Training Centre (DRTC). G.H.J. was supported by the Ontario Institute for Cancer Research (PanCuRx Translational Research Initiative) through funding provided by the Government of Ontario. The funding bodies had no role in study design, data collection, interpretation, or the decision to submit the work for publication.

Author contributions

SSWN, LAD: conceptual design of the study. IJK, YQ: GC/MS and LC/MS identification and quantification of plasma metabolites. SSWN, GHJ, IJK: data analysis, data interpretation. SSWN: manuscript writing. SSWN, GHJ, IJK, YQ, CG, LAD: critical reading of the manuscript. SSWN, LAD: overall supervision of the project.

Declaration of competing interest

The authors have no competing interest to declare.

Acknowledgement

We thank the patients who participated in this study.

Supplementary materials

Supplementary material associated with this article can be found, in the online version, at doi:10.1016/j.ebiom.2020.102973.

References

[1] Bujold A, Massey CA, Kim JJ, Brierley J, Cho C, Wong RKS, et al. Sequential phase I and II trials of stereotactic body radiotherapy for locally advanced hepatocellular carcinoma. J Clin Oncol 2013;31:1631–9.
[2] Sanuki N, Takeda A, Oku Y, Mizuno T, Aoki Y, Eriguchi T, et al. Stereotactic body radiotherapy for small hepatocellular carcinoma: a retrospective outcome analysis in 185 patients. Acta Oncol 2014;53:399–404.
[3] Yoon SM, Lim Y-S, Park MJ, Kim SY, Cho B, Shim JH, et al. Stereotactic body radiation therapy as an alternative treatment for small hepatocellular carcinoma. PLoS One 2013;8:e79854.
[4] Ohri N, Tomé WA, Méndez Romero A, Miften M, Ten Haken RK, Dawson LA, et al. Local control after stereotactic body radiation therapy for liver tumors. Int J Radiat Oncol Biol Phys 2018 S0360-3016(17)34525-X. doi: 10.1016/j.ijrobp.2017.12.288.
[5] Culleton S, Jiang H, Haddad CR, Kim J, Brierley J, Brade A, et al. Outcomes following definitive stereotactic body radiotherapy for patients with Child-Pugh B or C hepatocellular carcinoma. Radiother Oncol 2014;111:412–7.
[6] Munoz-Schuffenegger P, Ng S, Dawson LA. Radiation-induced liver toxicity. Semin Radiat Oncol 2017;27:350–7.
[7] Zhong J, Rajaram N, Brizel DM, Frees AE, Ramanujam N, Batinic-Haberle I, et al. Radiation induces aerobic glycolysis through reactive oxygen species. Radiother Oncol 2013;106:390–6.
[8] Dittmann K, Mayer C, Paasch A, Huber S, Fehrenbacher B, Schaller M, et al. Nuclear EGFR renders cells radio-resistant by binding mRNA species and triggering a metabolic switch to increase lactate production. Radiother Oncol 2015;116:431–7.
[9] Kurland IJ, Broin PÓ, Golden A, Su G, Meng F, Liu L, et al. Integrative metabolic signatures for hepatic radiation injury. PLoS One 2015;10:e0124795.
[10] Johnson PJ, Berhane S, Kagebayashi C, Satomura S, Teng M, Reeves HL, et al. Assessment of liver function in patients with hepatocellular carcinoma: a new evidence-based approach-the ALBI grade. J Clin Oncol 2015;33:550–8.
[11] Eisenhauer EA, Therasse P, Bogaerts J, Schwartz LH, Sargent D, Ford R, et al. New response evaluation criteria in solid tumours: revised RECIST guideline (version 1.1). Eur J Cancer 2009;45:228–47.
[12] Benjamini Y, Hochberg Y. Controlling the false discovery rate: a practical and powerful approach to multiple testing. J Royal Stat Soc: series B 1995;57:289–300.
[13] Benjamini Y, Yekutieli D. The control of the false discovery rate in multiple testing under dependency. Annals Stats 2001;29:1165–88.
[14] De Matteis S, Ragusa A, Marisi G, De Domenico S, Casadei Gardini A, Bonafè M, et al. Aberrant metabolism in hepatocellular carcinoma provides diagnostic and therapeutic opportunities. Oxid Med Cell Longev 2018;2018:7512159.
[15] Fitian AI, Nelson DR, Liu C, Xu Y, Ararat M, Cabrera R. Integrated metabolomic profiling of hepatocellular carcinoma in hepatitis C cirrhosis through GC/MS and UPLC/MS-MS. Liver Int 2014;34:1428–44.
[16] Chen S, Yin P, Zhao X, Xing W, Hu C, Zhou L, et al. Serum lipid profiling of patients with chronic hepatitis B, cirrhosis, and hepatocellular carcinoma by ultra fast LC/IT-TOF MS. Electrophoresis 2013;34:2848–56.
[17] Lu Y, Chen J, Huang C, Li N, Zou L, Chia SE, et al. Comparison of hepatic and serum lipid signatures in hepatocellular carcinoma patients leads to the discovery of diagnostic and prognostic biomarkers. Oncotarget 2018;9:5032–43.
[18] Patterson AD, Maurhofer O, Beyoglu D, Lanz C, Krausz KW, Pabst T, et al. Aberrant lipid metabolism in hepatocellular carcinoma revealed by plasma metabolomics and lipid profiling. Cancer Res 2011;71:6590–600.
[19] Han J, Qin W-X, Li Z-L, Xu A-J, Xing H, Wu H, et al. Tissue and serum metabolite profiling reveals potential biomarkers of human hepatocellular carcinoma. Clinica Chimica Acta 2019;488:68–75.
[20] Ridgway ND. The role of phosphatidylcholine and choline metabolites to cell proliferation and survival. Crit Rev Biochem Mol Biol 2013;48:20–38.
[21] Wu J-M, Xu Y, Skill NJ, Sheng H, Zhao Z, Yu M, et al. Autotaxin expression and its connection with the TNF-alpha-NF-kappaB axis in human hepatocellular carcinoma. Mol Cancer 2010;9:71.
[22] Cheema AK, Mehta KY, Rajagopal MU, Wise SY, Fatanmi OO, Singh VK. Metabolomic studies of tissue injury in nonhuman primates exposed to gamma-radiation. Int J Mol Sci 2019;20:3360–72.
[23] Wu H, Xu C, Gu Y, Yang S, Wang Y, Wang C. An improved pseudotargeted GC-MS/MS-based metabolomics method and its application in radiation-induced hepatic injury in a rat model. J Chromatogr B Analyt Technol Biomed Life Sci 2020;1152:122250–9.
[24] Cheema AK, Grindrod S, Zhong X, Jain S, Menon SS, Mehta KY, et al. Discovery of metabolic biomarkers predicting radiation therapy late effects in prostate cancer patients. Adv Exp Med Biol 2019;1164:141–50.
[25] Goossens C, Nahon P, Le Moyec L, Triba MN, Bouchemal N, Amathieu R, et al. Sequential serum metabolomic profiling after radiofrequency ablation of hepatocellular carcinoma reveals different response patterns according to etiology. J Proteome Res 2016;15:1446–54.
[26] Lee H-S, Shun C-T, Chiou L-L, Chen C-H, Huang G-T, Sheu J-C. Hydroxyproline content of needle biopsies as an objective measure of liver fibrosis: emphasis on sampling variability. J Gastroenterol Hepatol 2005;20:1109–14.